Published OnlineFirst December 17, 2010; DOI:10.1158/0008-5472.CAN-10-2350

Cancer Research

The Epithelial-Mesenchymal Transition Mediator S100A4 Maintains Cancer-Initiating Cells in Head and Neck Cancers

Jeng-Fan Lo, Cheng-Chia Yu, Shih-Hwa Chiou, et al.

Cancer Res 2011;71:1912-1923. Published OnlineFirst December 17, 2010.

Updated Version Access the most recent version of this article at: doi:10.1158/0008-5472.CAN-10-2350

Supplementary Material Access the most recent supplemental material at: http://cancerres.aacrjournals.org/content/suppl/2010/12/17/0008-5472.CAN-10-2350.DC1.html

Cited Articles This article cites 48 articles, 19 of which you can access for free at: http://cancerres.aacrjournals.org/content/71/5/1912.full.html#ref-list-1

E-mail alerts Sign up to receive free email-alerts related to this article or journal.

Reprints and Subscriptions To order reprints of this article or to subscribe to the journal, contact the AACR Publications Department at pubs@aacr.org.

Permissions To request permission to re-use all or part of this article, contact the AACR Publications Department at permissions@aacr.org.

Downloaded from cancerres.aacrjournals.org on March 23, 2011
Copyright © 2011 American Association for Cancer Research

Published OnlineFirst December 17, 2010; DOI:10.1158/0008-5472.CAN-10-2350

Tumor and Stem Cell Biology

Cancer Research

The Epithelial-Mesenchymal Transition Mediator S100A4 Maintains Cancer-Initiating Cells in Head and Neck Cancers

Jeng-Fan Lo[1–3], Cheng-Chia Yu[1,4], Shih-Hwa Chiou[1,5], Chih-Yang Huang[6–8], Chia-Ing Jan[9], Shu-Chun Lin[1], Chung-Ji Liu[10], Wen-Yuan Hu[11], and Yau-Hua Yu[1,2,5]

Abstract

Cancer-initiating cells (CIC) comprise a rare subpopulation of cells in tumors that are proposed to be responsible for tumor growth. Starting from CICs identified in head and neck squamous cell carcinomas (HNSCC), termed head and neck cancer-initiating cells (HN-CIC), we determined as a candidate stemness-maintaining molecule for HN-CICs the proinflammatory mediator S100A4, which is also known to be an inducer of epithelial-mesenchymal transition. S100A4 knockdown in HN-CICs reduced their self-renewal capability and their stemness and tumorigenic properties, both *in vitro* and *in vivo*. Conversely, S100A4 overexpression in HNSCC cells enhanced their stem cell properties. Mechanistic investigations indicated that attenuation of endogenous S100A4 levels in HNSCC cells caused downregulation of Notch2 and PI3K (phosphoinositide 3-kinase)/pAKT along with upregulation of PTEN, consistent with biological findings. Immunohistochemical analysis of HNSCC clinical specimens showed that S100A4 expression was positively correlated with clinical grading, stemness markers, and poorer patient survival. Together, our findings reveal a crucial role for S100A4 signaling pathways in maintaining the stemness properties and tumorigenicity of HN-CICs. Furthermore, our findings suggest that targeting S100A4 signaling may offer a new targeted strategy for HNSCC treatment by eliminating HN-CICs. *Cancer Res; 71(5); 1912–23. ©2010 AACR.*

Introduction

Accumulating data support the hierarchical model of cancer-initiating cells (CIC) or cancer stem cells (CSC) in that each tumor formation is governed by a rare subpopulation of cells with self-renewal capacity (1, 2). CICs have been shown to have capacities of promoting tumor growth, tumor regeneration, metastatic progression, and contributing to radioresistance and chemoresistance (3, 4). We previously enriched a subpopulation of head and neck cancer-initiating cells (HN-CIC) from head and neck squamous cell carcinoma cells (HNSCC) by sphere formation assay (5). The enriched HN-CICs possess the properties of both stemness and malignant tumors. However, it is still elusive with regard to the molecular mechanistic understanding, leading to the phenotypic properties of HN-CICs.

Epithelial-mesenchymal transition (EMT), a process by which epithelial cells lose their polarity and later acquire a migratory mesenchymal phenotype, is one of the crucial processes that induce tumor invasion and metastasis (6). Researchers have shown that EMT could promote stem cell (SC) properties and further generate cells with the features of breast CSCs (7–9). Therefore, the study of how modulators of EMT processes operate or manifest the stem-like properties and the tumorigenicity of HN-CICs is warranted to shed light for future research.

S100A4, a member of calcium-binding proteins, is directly controlled by Wnt/β-catenin signaling pathway as a master mediator in EMT (10). Involved in a variety of biological effects including cell motility, survival, differentiation, and cytoskeletal organization (11–14), S100A4 was also shown to play an important role in both stem cell and cancer biology. For instance, S100A4 is considered to be a normal stemness marker and plays a crucial role in the self-renewal of bulge stem cells (11, 13, 14). Mice lacking *S100A4* gene suppresses the tumor development and metastasis (15). S100A4 is also established as a regulator of metastasis, while it is ectopically overexpressed in tumor cells where, consequently, it promotes the metastatic phenotype (16, 17). In contrast, inhibition of S100A4 expression reduces the metastatic capacity of tumor cells (18). Recent data point out that S100A4 is highly expressed in human embryonal carcinoma cells but not in

Authors' Affiliations: [1]Institute of Oral Biology and [2]Department of Dentistry, National Yang-Ming University; [3]Department of Dentistry, Taipei Veterans General Hospital, Taipei; [4]Institute of Oral Biology and Biomaterial Science, Chung-Shan Medical University, Taichung; [5]Department of Medical Research and Education, Taipei Veterans General Hospital, Taipei; [6]Graduate Institute of Chinese Medical Science and Institute of Medical Science; [7]Institute of Basic Medical Science, China Medical University; [8]Department of Health and Nutrition Biotechnology, Asia University; [9]Department of Pathology, China Medical University and Hospital, Taichung; [10]Department of Oral and Maxillofacial Surgery, Mackay Memorial Hospital, Taipei, Taiwan, ROC; and [11]Biosettia Inc., San Diego, California

Note: Supplementary data for this article are available at Cancer Research Online (http://cancerres.aacrjournals.org/).

Corresponding Author: Jeng-Fan Lo, Institute of Oral Biology, National Yang-Ming University, No. 155, Section 2, Li-Nung Street, Taipei, 11217, Taiwan, ROC. Phone: 886-2-28267222; Fax: 886-2-28264053; E-mail: jflo@ym.edu.tw

doi: 10.1158/0008-5472.CAN-10-2350

©2010 American Association for Cancer Research.

Downloaded from cancerres.aacrjournals.org on March 23, 2011
Copyright © 2011 American Association for Cancer Research

Published OnlineFirst December 17, 2010; DOI:10.1158/0008-5472.CAN-10-2350

human embryonic stem cells (ESC) by a comprehensive quantitative proteomic analysis (19). In addition, S100A4 is significantly upregulated in mouse glioma CSCs (20). Others have shown the prognostic significance of S100A4 in many solid tumors including breast cancer, colon cancer, and bladder cancer (21–23). However, the role of S100A4 in HNSCC has not been well characterized.

Herein, we show that alteration of S100A4 expression affects CICs properties in HNSCCs. In addition, immunoactivity of S100A4 on HNSCC tumor tissues correlates with clinical grading, survivals, and stemness markers. Thus, our study implicated that S100A4 played an important role in the pathogenesis of HNSCC and S100A4 might be a potential therapeutic target for HNSCC.

Materials and Methods

Cell lines cultivation and enrichment of HN-CICs from HNSCCs

Two well-established HNSCC cell lines (SAS and OECM1) and 1 primary HNSCC cell line, used in this research, were derived from HNSCCs (5). In brief, originally, SAS and primary HNSCC were grown in Dulbecco's modified Eagle's medium (DMEM), and OECM1 was grown in RPMI supplemented with 10% FBS, respectively. For enrichment of HN-CICs, the above 3 cell lines were then cultured in tumor sphere medium consisting of serum-free DMEM/F12 medium (GIBCO), N2 supplement (GIBCO), 10 ng/mL human recombinant basic fibroblast growth factor, and 10 ng/mL epidermal growth factor (R&D Systems; ref. 24).

Microarray differential expression analysis

Gene profiling was done using Affymetrix Human Genome U133plus2.0. All CEL files were preprocessed using "justRMA" and standardized with mean = 0 and SD = 1. The fuzzy c-mean (FCM) algorithms of "Mfuzz" package was used to analyze temporal gene expression patterns of our SAS HN-CICs (25). We focused the analysis on 63 EMT-related genes (204 probe sets). Parameters in FCM were set as suggested ($m = 1.25$; $c = 6$; ref. 25). Functional annotation of gene clusters was carried out with the Web-based program of DAVID (Database for Annotation Visualization and Integrated Discovery; ref. 26). Modified t test of "limma" package (27) was used for differential gene expression analysis between the control- or S100A4-knockdown HN-CICs, controlled for false discovery rate (FDR) < 0.05 (28). Two manually curated gene sets were used: 1999 EMT and calcium signaling-related genes (4,235 probe sets, EMT-Calcium; ref. 29) and, 3,939 stemness genes (8,606 probe sets, ESC; refs. 30, 31).

Network analysis of human protein–protein interactions

Perturbed genes after small hairpin RNA interference (shRNAi)–mediated knockdown of S100A4 were mapped in the protein–protein interactions downloaded from the Human Protein Reference Database (32). Interactions would be mapped only when both of the interacting genes were listed in the EMT-Calcium or ESC sets. Topological characteristics were examined among the first- and second-order connecting neighbors of the mapped genes, that is, subnetworks of the shortest path of a maximum of 3 between any pair of these significantly perturbed genes (29). Analytical analyses were done in R environment (33) and displayed by Cytoscape (34).

Aldehyde dehydrogenase activity analysis

Aldehyde dehydrogenase activity was examined with ALDEFLUOR kit (Stem cell Technologies) and was done according to manufacturer's guidelines (35).

Side population analysis

Cells were resuspended at 1×10^6/mL in prewarmed DMEM with 2% FCS. Hoechst 33342 dye was added at a final concentration of 5 μg/mL in the presence or absence of verapamil (50 μmol/L; Sigma) and was incubated at 37°C for 90 minutes. The cells were then washed with ice-cold HBSS with 2% FCS. Propidium iodide at a final concentration of 2 μg/mL was added to the cells to gate viable cells. The Hoechst 33342 dye was excited at 357 nm and its fluorescence was dual-wavelength analyzed (blue, 402–446 nm; red, 650–670 nm). Analyses were done on a FACSVantage system (BD Biosciences).

Subcutaneous xenografts in nude mice

All the animal practices in this study were in accordance with the institutional animal welfare guideline of Taipei Veterans General Hospital (VGH), Taiwan. Cells were injected subcutaneously into BALB/c nude mice (6–8 weeks). Tumor volume (TV) was calculated using the following formula: TV (mm^3) = (Length × Width^2)/2 and then analyzed using Image Pro-Plus software.

Patient subjects and immunohistochemistry

Between 1994 and 1997, 102 patients with operable head and neck cancer, without histories of radiation or chemotherapy, underwent surgery at the Department of Oral and Maxillofacial Surgery, Mackay Memorial Hospital. This research follows the tenets of the Declaration of Helsinki, and all samples were obtained after informed consent from the patients. Patients' tissue samples with different stages of oral cancer were spotted on glass slides for immunohistochemical staining (Supplementary Table S1). After deparaffinization and rehydration, antigen retrieval was processed within 1X-Trilogy buffer (Biogenics). The slides were immersed in 3% H_2O_2 for 10 minutes, washed, and then blocked with serum (Vestastain Elite ABC kit; Vector Laboratories), followed by incubation with the primary anti-S100A4 antibody (code no. A5114; Dako; refs. 36–38). Tissue slides were then stained with biotin-labeled secondary antibody and incubated with streptavidin–horse radish peroxidase conjugates. Afterward, the tissue sections were immersed with chromogen 3,3′-diaminobenzidine plus H_2O_2 substrate solution (Vector DBA/Ni substrate kit, SK-4100; Vector Laboratories). Hematoxylin was applied for counterstaining (Sigma Chemical Co). Pathologists scoring the immunohistochemistry (IHC) were blinded to the clinical data. The interpretation was done in 5 high-power views for each slide, and 100 cells per view were counted for analysis.

Downloaded from cancerres.aacrjournals.org on March 23, 2011
Copyright © 2011 American Association for Cancer Research

Published OnlineFirst December 17, 2010; DOI:10.1158/0008-5472.CAN-10-2350

Statistical analysis

Statistical package of social sciences software (version 13.0; SPSS Inc.) was used for statistical analysis. The independent Student's t test or ANOVA was used to compare the continuous variables between groups, whereas the χ^2 test was applied for the comparison of dichotomous variable. The Kaplan–Meier estimate was used for survival analysis, and the log-rank test was selected to compare the cumulative survival durations in different patient groups. The level of statistical significance was set at 0.05 for all tests.

Results

Elevated expression of S100A4 in HN-CICs

Cells undergoing EMT processes promote the gain of stem-like properties in breast carcinoma cells (8, 9). Therefore, we were interested in knowing whether EMT-related genes were differentially expressed in the enriched HN-CICs from SAS cells under 2, 3, 5, and 9 weeks of cultivation within defined serum-free selection medium. We observed a clear separation of EMT-related gene expression patterns in 6 clusters without redundancy (Fig. 1A and B and

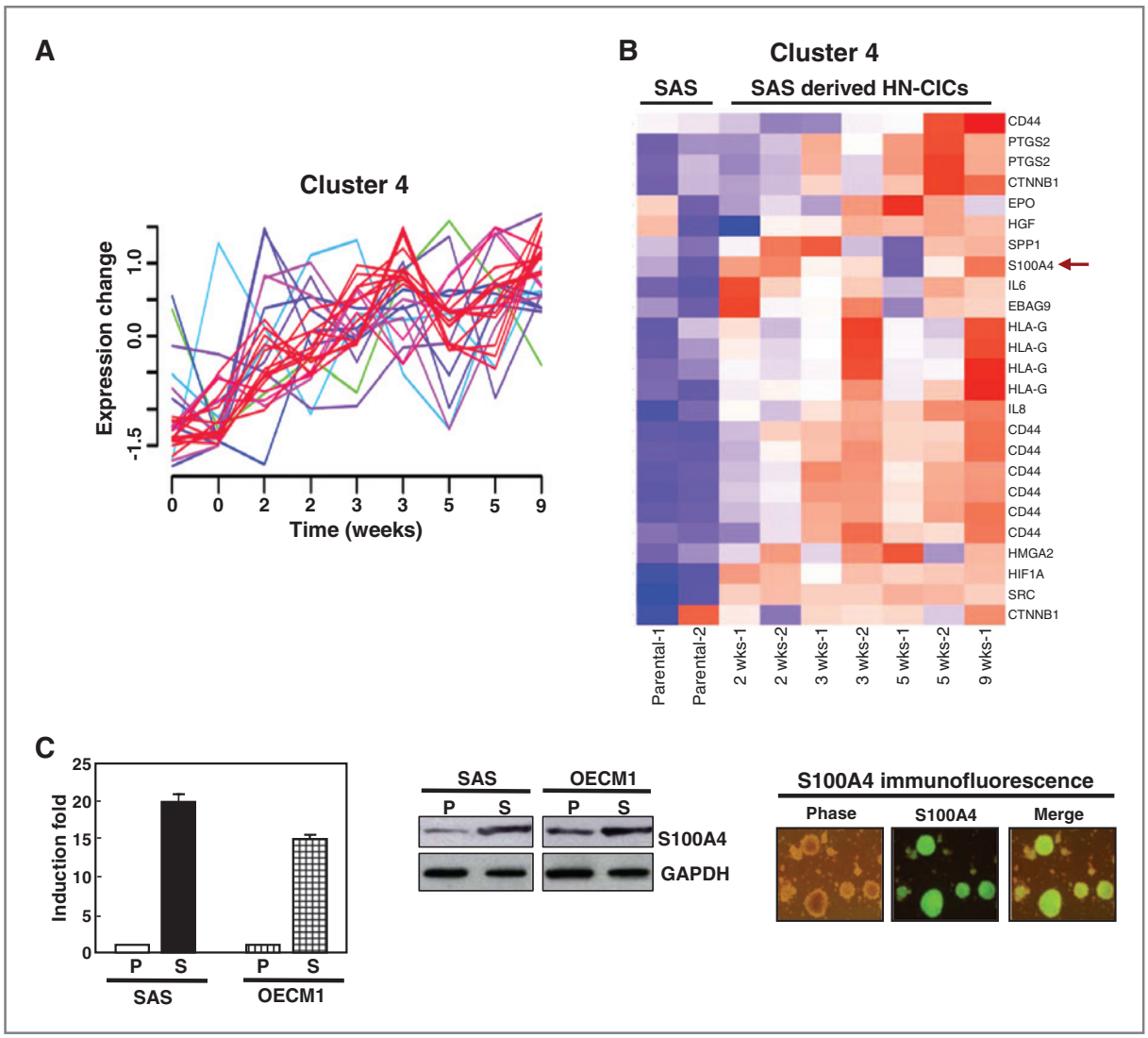

Figure 1. Expression profiles of EMT-related genes in enriched HN-CICs. The differential transcriptome profiles between SAS cells and SAS-derived HN-CICs under 2, 3, 5, or 9 weeks of cultivation with defined serum-free selection medium were collected and analyzed. A, cluster 4 differential gene expression profile. B, the heat maps of the cluster 4 transcripts. Red and blue indicate high and low expression levels, respectively. C, the expression of S100A4 transcript in parental HNSCCs (SAS and OECM1) or derived HN-CICs was detected by real-time RT-PCR analysis (data are means ± SD of triplicate samples from 3 experiments; left). Protein level of S100A4 and glyceraldehyde 3-phosphate dehydrogenase (GAPDH) in parental HNSCC or HN-CIC cells were analyzed by immunoblotting (middle). Intracellular localization of S100A4 of enriched HN-CICs was examined by immunofluorescence. Magnification, ×200 (right).

Downloaded from cancerres.aacrjournals.org on March 23, 2011
Copyright © 2011 American Association for Cancer Research

Published OnlineFirst December 17, 2010; DOI:10.1158/0008-5472.CAN-10-2350

Table 1. Functional annotation of cluster 4

Cluster	Number of probes	Functional annotation	Geometric mean of *P*-values	Modified fisher exact *P*-value
4	25	GO:0001837~epithelial to mesenchymal transition	3.45E-4	6.02E-09
		GO:0048762~mesenchymal cell differentiation		7.42E-08
		GO:0014031~mesenchymal cell development		7.42E-08
		GO:0048468~cel development		0.002571

Supplementary Figs. S1A and S2A). Cluster 4 showed a significant increasing trend of gene activities (Fig. 1A). S100A4, a well-known player in the EMT and metastasis processes, was identified in cluster 4 showing induced activities in HN-CICs (Fig. 1A and B). Functional annotation of cluster 4 showed enrichment in EMT, mesenchymal cell differentiation, and cell development (Table 1). Empirically, the amount of S100A4 transcripts of enriched HN-CICs derived from both SAS and OECM1 HNSCCs were significantly increased in comparison with that of the parental HNSCCs, by either real-time PCR (Fig. 1C, left panel) or reverse transcriptase PCR (RT-PCR) analysis (Supplementary Fig. S1B). Accordingly, the Western blotting data showed that the protein levels of S100A4 in enriched HN-CICs were also upregulated (Fig. 1C, middle panel). Furthermore, immunofluorescent staining displayed that the intracellular levels of S100A4 in the tumor spheres derived from SAS cells were dramatically increased (Fig. 1C, right panel).

Effect of S100A4 knockdown on HNSCC and HN-CICs

To further investigate the crucial role of S100A4 upregulation in maintaining the biological properties of HN-CICs, we conducted loss-of-function approach by shRNAi-mediated knockdown of S100A4 in HNSCCs. Stable S100A4 knockdown in SAS, primary HNSCC, and OECM1 cells was achieved by transduction with lentivirus-expressing shRNA targeting S100A4 (Sh-S100A4-1 and Sh-S100A4-2), and lentivirus-expressing shRNA against luciferase (Sh-Luc) was used as a control. The amount of S100A4 transcript was significantly decreased in stable S100A4-knockdown HNSCCs by real-time PCR analyses (Supplementary Fig. S3A, left panels). Western blot analysis further confirmed that both Sh-S100A4-1 and Sh-S100A4-2 markedly reduced S100A4 protein expression in both HNSCCs (SAS and primary HNSCC cells; Fig. 2A, left panels).

As successful sphere formation of CSCs under serial passages is a key behavior of normal SCs and CSCs for evaluating *in vitro* self-renewal property (39), we then determined the sphere formation capacity of HNSCCs with stable S100A4 knockdown. Knockdown of S100A4 markedly decreased the ability of HNSCCs to form tumor spheres (Supplementary Fig. S3A, right panels) and was indicated by the reduction in sphere formation efficiency after serial passages (Fig. 2A, right panels). In addition, the enzymatic activity of aldehyde dehydrogenase (ALDH), which has been identified as a CSC marker (35), was also significantly reduced in HNSCCs with S100A4 downregulation (Fig. 2B, left panels). It has been shown that tumor-derived side population (SP) cells display the characteristics of cancer stem cells (40). Here, we showed that S100A4 depletion significantly decreased the SP in primary HNSCC and OECM1 cells (Fig. 2B, middle and right panels; Supplementary Fig. S3B, left panels). Furthermore, stable S100A4 knockdown also decreased ABCG2-positive cells in which high expression of ABCG2 possibly contributes to SP phenotype and drug resistance in many cancers (Supplementary Fig. S3B, right panels; ref. 41). In addition, stable S100A4-knockdown HNSCCs also dramatically decreased "cancer stemness" genes (*Oct-4* and *Nanog*) expression (Supplementary Fig. S3C).

To further investigate whether S100A4 expression plays a role in maintaining self-renewal or cancer stem-like properties of HN-CICs directly, the SAS or primary HNSCC-derived tumor spheres, afterward, transduced with Sh-S100A4 lentivirus, did not maintain floating spheres but showed more attached epithelial-like cells (Fig. 2C). Instead, tumor spheres after Sh-S100A4 lentiviruses infection displayed enhanced expression of epithelial differentiation marker, CK18 (Fig. 2D, left and middle panels), and also decreased "cancer stemness" genes (*Oct-4* and *Nanog*) expression (Supplementary Fig. S3D). To determine whether the reduction in tumor sphere formation efficiency with S100A4 downregulation is due to decreased HN-CIC survival, we determined the percentage of apoptotic cells by Annexin V staining. Primary HNSCC or SAS-derived HN-CICs transduced with Sh-S100A4 lentivirus significantly increased the percentage of Annexin V–positive cells (Fig. 2D, right panel; data not shown). Together, these data further support that the depletion of S100A4 resulted in a reduction of CICs population in HNSCCs.

The cell migratory/invasion/colony formation abilities of HNSCCs (SAS and OECM1) with stable S100A4 knockdown were also significantly reduced (Supplementary Fig. S4A–C). Furthermore, stable S100A4 knockdown abrogated EMT signatures with upregulation of E-cadherin and downregulation of vimentin by immunoblotting analyses (Supplementary Fig. S4D).

Downloaded from cancerres.aacrjournals.org on March 23, 2011
Copyright © 2011 American Association for Cancer Research

Published OnlineFirst December 17, 2010; DOI:10.1158/0008-5472.CAN-10-2350

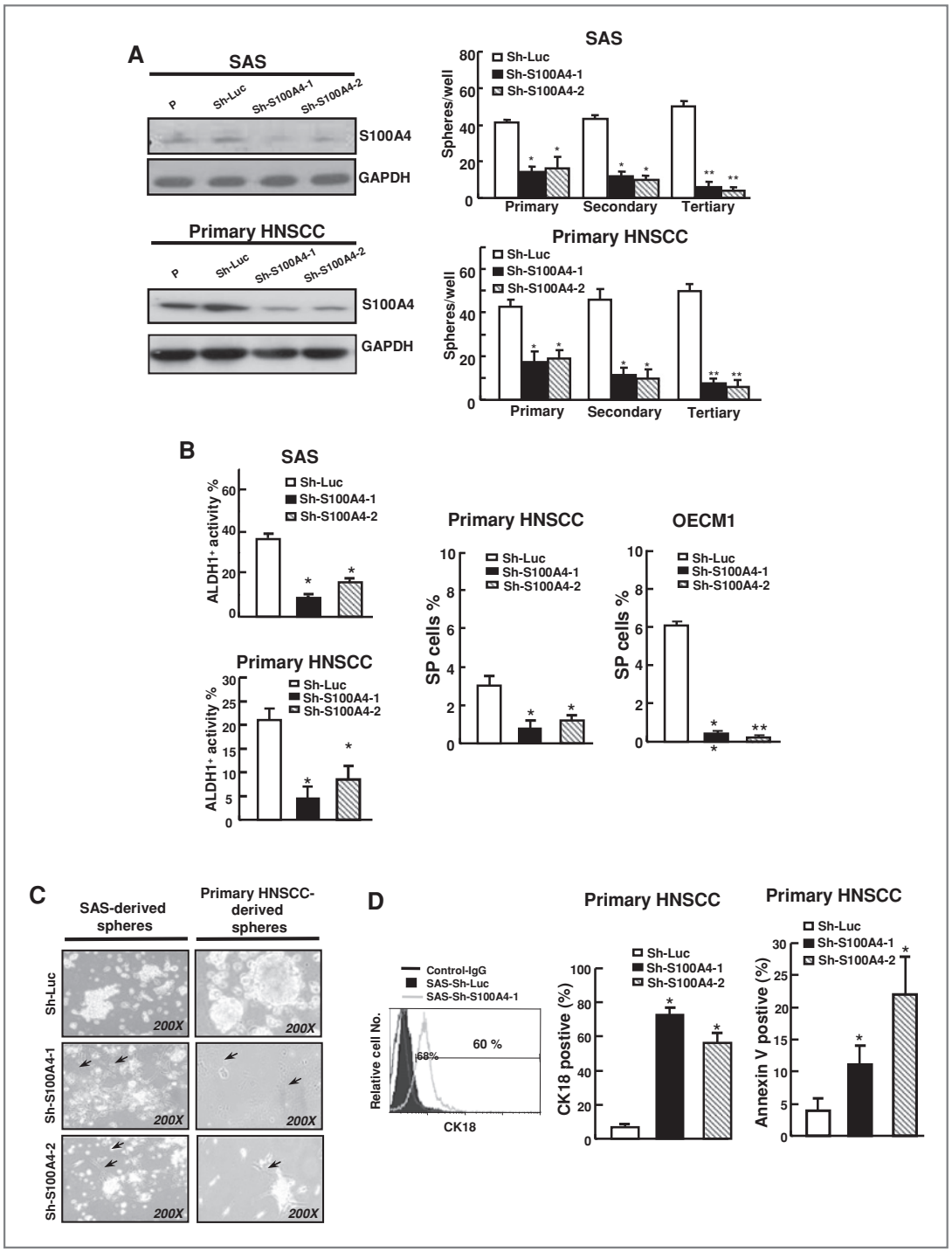

Figure 2. Depletion of S100A4 impairs self-renewal and stemness properties but enhances cell differentiation and apoptosis of HN-CICs. A, protein level of S100A4 in stable S100A4-knockdown (Sh-S100A4-1 or Sh-S100A4-2) HNSCCs (SAS and primary HNSCC) was detected by Western blotting (left, top and bottom). Stable S100A4-knockdown HNSCCs were grown under defined serum-free selection medium for primary spheres formation and then serial passage spheres, including secondary sphere and tertiary sphere established from primary sphere after every 3 weeks of incubation, were generated. The numbers of primary spheres, secondary spheres, and tertiary spheres of SAS or primary HNSCC cells with stable S100A4 knockdown were calculated, respectively (right top and bottom).*, $P < 0.05$; **, $P < 0.01$. B, the ALDH enzymatic activity of Sh-S100A4 and control (Sh-Luc) HNSCCs (SAS and primary HNSCC) were examined. SP cells of primary HNSCC (middle) or OECM1 (right) in Sh-S100A4 and control OECM1 cells were examined, respectively.*, $P < 0.05$; **, $P < 0.01$. C, SAS or primary HNSCC-derived HN-CICs infected with Sh-S100A4-1, Sh-S100A4-2, or Sh-Luc lentivirus were further cultivated under the serum-free defined selection medium, and the cellular morphology of virus infected cells were observed. Arrows indicate the attached epithelial-like cells. D, representative expression profile of CK18 in HN-CIC cells [SAS (left) and primary HNSCC (middle)] infected with Sh-Luc or Sh-S100A4-1 lentivirus was assessed by fluorescence activated cell sorting. Single cell from primary HNSCC cells was stained with Annexin V (right). Results are means ± SD of triplicate samples from 3 experiments. *, $P < 0.05$; **, $P < 0.01$.

Downloaded from cancerres.aacrjournals.org on March 23, 2011
Copyright © 2011 American Association for Cancer Research

Published OnlineFirst December 17, 2010; DOI:10.1158/0008-5472.CAN-10-2350

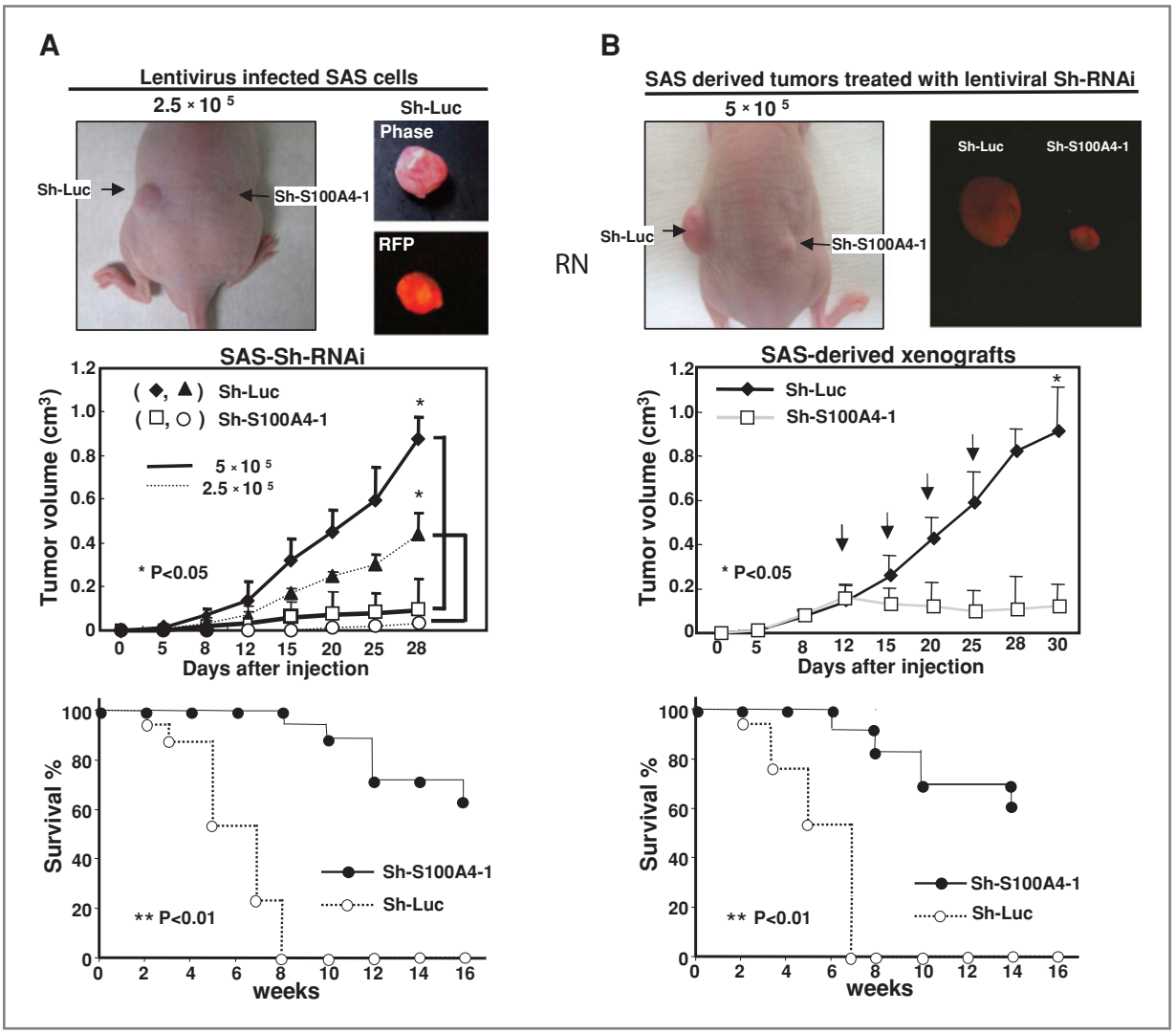

Figure 3. Knockdown of S100A4 attenuates HNSCC xenograft tumor growth. A, representative tumor growth of control SAS cells (SAS-Luc: 2.5 × 10^5) or S100A4-knockdown SAS cells (top). Tumor volume was measured after inoculation of Sh-S100A4-1 or Sh-Luc–expressing cells. Error bars correspond to SD (middle). The survival curves of mice injected with the Sh-S100A4-1 cells (solid circle with solid line) or Sh-Luc cells (open circle with dash line) were recorded (bottom). B, parental SAS cells (5 × 10^5 cells) were subcutaneously implanted into left and right back of nude mice and allowed to develop tumors to a size around 0.2 cm^3 (12 days). On days 12, 15, 20, and 25 after implantation, progressively growing SAS-derived tumors were subject to Sh-Luc or Sh-S100A4-1 lentivirus as arrows indicate and were recorded, respectively. A representative result of tumor growth on nude mice; red fluorescence indicates the red fluorescent protein (RFP) reporter signal (top). Tumor volume was measured after inoculation of parental SAS cells and injection of lentiviruses expressing control viruses or Sh-S100A4-1 lentivirus. Error bars correspond to SD (middle). The survival curves of tumor-bearing nude mice treated with the Sh-S100A4-1 or Sh-Luc lentivirus were recorded (bottom).

Downregulation of S100A4 attenuates tumorigenicity of HNSCCs *in vivo*

We next sought to determine whether downregulation of S100A4 expression reduces the tumor-forming ability of HNSCCs *in vivo*. As shown in Table 2, SAS control cells generated tumor when 2.5 × 10^5 cells were injected into nude mice (6/6 mice); however, stable S100A4-knockdown SAS cells inefficiently gave rise to a new tumor at the injection of 5 × 10^5 cells in 1 of 6 mice. In addition, knockdown of S100A4 in SAS cells significantly reduced the tumor volumes (Fig. 3A, top and middle panels; $^*P < 0.05$) and prolonged the survival of nude mice (Fig. 3A, bottom panel; $^{**}P < 0.01$). Our data indicate that downregulation of S100A4 diminished

Table 2. Tumorigenicity of SAS-Sh-Luc and SAS-Sh-S100A4 Cells in Nude Xenotransplant Assay

	Cell Numbers for Injection			
	2×10^6	1×10^6	5×10^5	2.5×10^5
SAS-Sh-Luc	6/6	6/6	6/6	6/6
SAS-Sh-S100A4-1	2/6	2/6	1/6	0/6

Summary of the *in vivo* tumor growth ability of stable S100A4-knockdown and Sh-Luc SAS cells examined by xenotransplantation

Downloaded from cancerres.aacrjournals.org on March 23, 2011
Copyright © 2011 American Association for Cancer Research

Published OnlineFirst December 17, 2010; DOI:10.1158/0008-5472.CAN-10-2350

the tumorigenicity of HNSCCs. Next, we addressed whether targeting S100A4 could represent a potential therapeutic treatment. We first injected parental SAS cells into nude mice and then allowed the tumors to be established for 12 days. Tumor-bearing mice were then injected intratumorally with lentivirus-expressing either Sh-Luc as a control or Sh-S100A4 as a therapeutic treatment target. Apparently, tumor-bearing mice receiving lentivirus-expressing Sh-S100A4 displayed retarded tumor growth (Fig. 3B, top panel and middle panels; $*P < 0.05$) and prolonged lifespan (Fig. 3B, bottom panel; $**P < 0.01$).

Overexpression of S100A4 in HNSCCs enhances stemness properties and tumorigenic potentials

To evaluate whether overexpression of S100A4 could enhance the stemness and tumorigenic properties of HNSCCs, we generated stable S100A4-overexpressing HNSCCs through lentiviral-mediated transduction. Total proteins from S100A4-overexpressing HNSCCs displayed elevated expression of S100A4 and vimentin but decreased expression of E-cadherin (Fig. 4A, left panel). The S100A4-overexpressing HNSCCs also showed significantly enhanced tumor sphere-forming capacity, both in size and in number, within 2 weeks of cultivation under defined serum-free medium (Fig. 4B and Supplementary Fig. S5A). Moreover, S100A4-overexpressing HNSCCs, under cultivation with defined serum-free medium for 2 weeks, displayed increased protein level of Oct-4 and Nanog (Fig. 4C). The S100A4-overexpressing HNSCCs also displayed significantly increased SP cells (Fig. 4D and Supplementary Fig. S5B). Furthermore, we showed that S100A4 overexpression also resulted in increased ability on *in vitro* cell migration (Supplementary Fig. S5C) and cell invasion (Supplementary Fig. S5D). Collectively, these results suggest that S100A4 overexpression promotes stemness properties and *in vitro* tumorigenicity of HNSCCs.

S100A4 IHC study in HNSCC patients

The expression profile of S100A4 in oral squamous cell carcinoma (OSCC) has been evaluated with controversial results (42, 43). The mRNA level of S100A4 is significantly downregulated in 27 cases of OSCCs/their pairwise normal controls obtained from Sudanese patients (43). However, Moriyama-Kita and colleagues showed the positive correlation of S100A4 expression with invasion and metastasis in 41 primary OSCC tissues of Japan patients (42). The controversy could be the result of different patient populations or sample sizes.

To thoroughly investigate the expression profile of S100A4 during the development of head and neck cancers in HNSCC patients, we established the ontogeny of S100A4 expression by tissue immunohistochemical staining with a panel of specimen array of 102 HNSCC patients. The

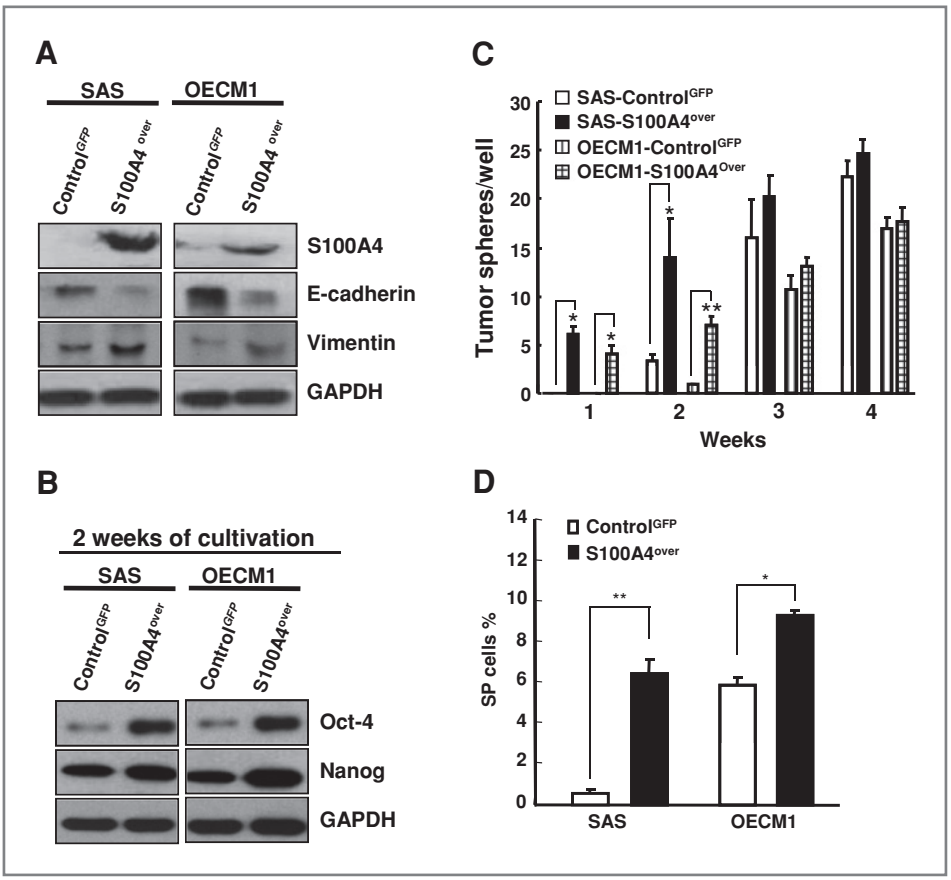

Figure 4. Overexpression of S100A4 enhances expression of EMT markers, stemness properties, and *in vitro* tumorigenic potentials of HNSSCs. A, total proteins were prepared from control or S100A4-overexpressing HNSCCs and analyzed by immunoblotting against anti–E-cadherin, anti-vimentin, or anti-GAPDH antibodies as indicated. B, total proteins of control or S100A4-overexpressing HNSCCs, after 2 weeks of cultivation under serum-free defined medium, were isolated and immunoblotted against anti–Oct-4 and anti-Nanog (right). C, the tumor sphere formation efficiency of control-green fluorescent protein and S100A4-overexpressing HNSCCs (SAS and OECM1) under serum-free defined medium for 1, 2, 3, or 4 weeks were calculated. D, SP cells of stable S100A4-overexpressing and control Sh-GFP–expressing HNSCCs were analyzed. Results are means ± SD of triplicate samples from 3 representative experiments. *, $P < 0.05$; **, $P < 0.01$.

Downloaded from cancerres.aacrjournals.org on March 23, 2011
Copyright © 2011 American Association for Cancer Research

Published OnlineFirst December 17, 2010; DOI:10.1158/0008-5472.CAN-10-2350

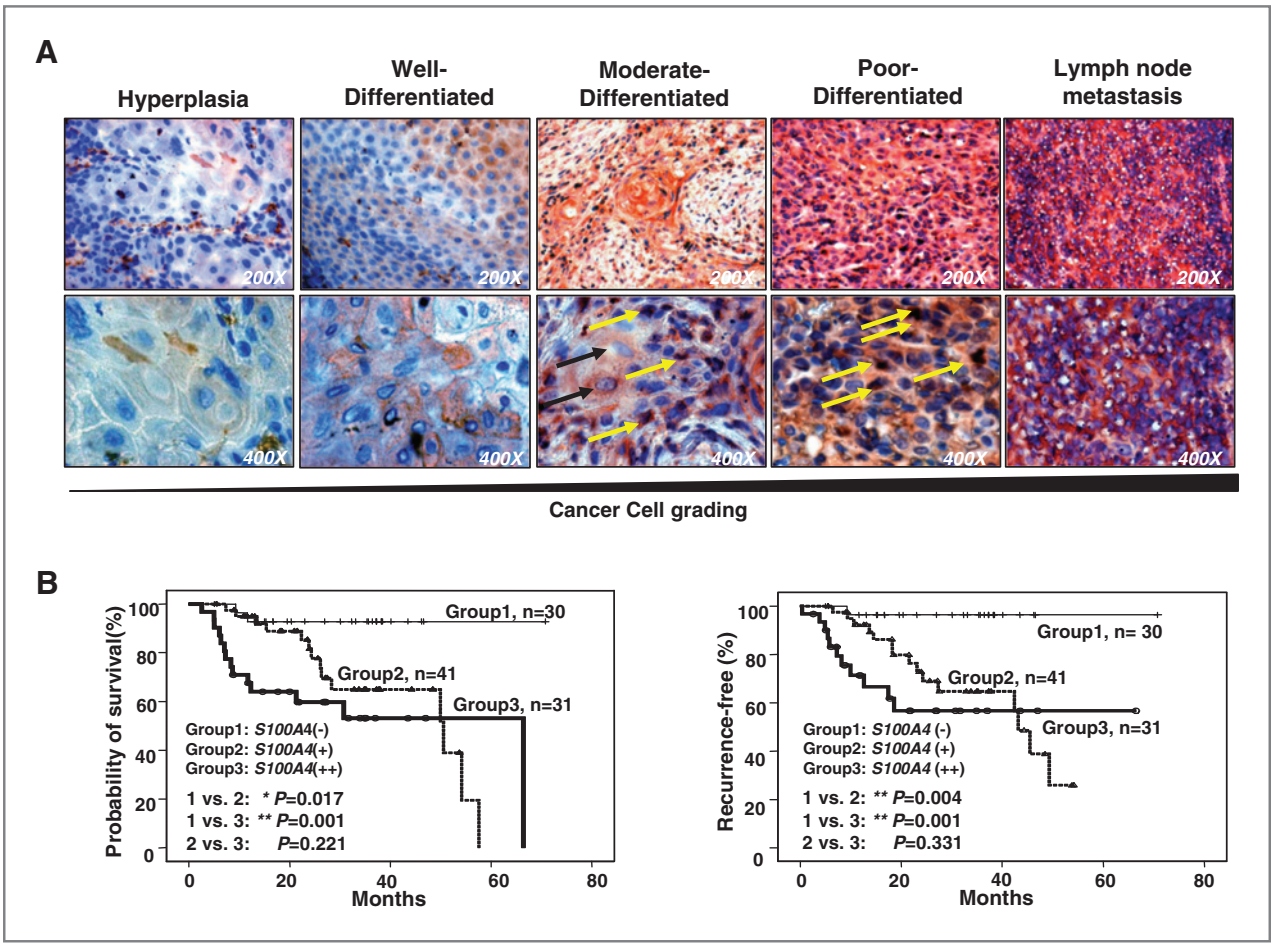

Figure 5. Correlation of S100A4 expression to clinical grading, predicted survival rate, and stemness markers of HNSCC patients. A, representative results of IHC staining of S100A4 on HNSCC patients with different stages are shown. Arrows indicate the positive staining of S100A4 (black arrows, cytoplasmic staining; yellow arrows, nucleus staining). Magnification is shown at bottom right corner. B, Kaplan–Meier analysis of overall survival (left) and recurrence status (right) in 102 HNSCC patients according to the expression of S100A4 (−, 0%–10% S100A4-positive cells; +, 10%–50% S100A4-positive cells; ++, more than 50% S100A4-positive cells; *, $P < 0.05$; **, $P < 0.01$).

clinicopathologic features of the subjects are summarized in Supplementary Table 1. We observed that elevated expression of S100A4 was highly correlated with medium to poor differentiation ($P < 0.0001$), tumor stage ($P < 0.0001$), lymph node metastasis ($P < 0.0001$), and advanced staging ($P < 0.0001$) of head and neck cancers (Fig. 5A and Table 3). In addition, we found more nuclear and cytoplasmic staining of S100A4 in the moderately to poorly differentiated HNSCC tissues than those of well-differentiated HNSCC tissues (Fig. 5A).

Poor overall survival rate and high recurrence of HNSCC patients were positively associated with S100A4 expression

To determine the prognostic significance of S100A4 expression in patients with HNSCC, Kaplan–Meier survival analyses were carried out. These analyses showed that an overall worse survival rate was associated with the S100A4 IHC-positive patients in comparison with the negative ones (Fig. 5B, left panel). In addition, HNSCC patients with intense S100A4 expression were also associated with greater recurrence status (Fig. 5B, right panel). Together, these results show a significantly positive correlation between higher expression of S100A4 and tumor progression in HNSCC.

Coexpression profile between S100A4 and stemness markers, Nanog, Oct-4, and CD133, of HNSCC

Furthermore, we wanted to understand the expression relationship between S100A4 and the known stemness markers (Nanog, Oct-4, and CD133) from our previous findings on HNSCC (5). Of the 34 HNSCC patients' tumorous tissues, which were previously immunohistochemically stained with Nanog, Oct-4, or CD133, respectively (5), we observed the significant coexpression between S100A4 and Nanog ($P < 0.001$; Table 4) and S100A4 and Oct-4 (Table 4, $P < 0.05$) but not in S100A4 and CD133 (Table 4, $P = 0.138$), with further staining against S100A4 antibodies.

Downloaded from cancerres.aacrjournals.org on March 23, 2011
Copyright © 2011 American Association for Cancer Research

Published OnlineFirst December 17, 2010; DOI:10.1158/0008-5472.CAN-10-2350

Table 3. Table of S100A4 expression and clinicopathologic variables in 102 HNSCC patients

Variables	($n = 102$)	− (%)	+ (%)	++ (%)	*P*
Age					
≥ 54	38	9 (24)	18 (47)	11 (29)	0.472
< 54	64	21 (33)	23 (36)	20 (31)	
Differentiation					
Well	39	18 (46)	19 (49)	2 (5)	
Moderate to Poor	63	12 (19)	22 (35)	29 (46)	****$P < 0.001$
T-stage					
Precancer-II	29	18 (62)	6 (21)	5 (17)	
T3-T4	73	12 (16)	35 (48)	26 (36)	****$P < 0.001$
Lymph node Metastasis					
$N = 0$	57	29 (51)	28 (49)	0 (0)	
$N \geq 1$	45	1 (2)	13 (29)	31 (69)	****$P < 0.001$
Stage					
Precancer-II	20	16 (80)	4 (20)	0 (0)	
III-IV	82	14 (17)	37 (45)	31 (38)	****$P < 0.001$

Note: Chi-Square test. (−, 0–10% positive cells; +, 10–50% positive cells; more than 50% positive cells).

S100A4 knockdown causes significant changes of calcium signaling, EMT, ESC, and developmental (*Notch2*) and cell survival (*PTEN*/*PI3K*/*Akt*)-related transcriptomes

By examining transcriptomic changes after shRNAi-mediated knockdown of S100A4 in HNSCCs, 35 genes in EMT-Calcium (Supplementary Fig. S6A) and 78 genes in ESC gene sets (Supplementary Fig. S6B) were perturbed. Interrelationships among the perturbed genes were mapped in the human protein-protein interactions (Fig. 6A). S100A4, with 14 neighbors in the EMT-Calcium networks, was the only connecting hub for *MYH4*, *SEPT*, and *PPFIBP1* (Fig. 6A, inset). *ACTA1*, *TPM3*, and *TP53* were also highly connected (Fig. 6A, inset). Network topological analysis among the first- and second-order neighbors of the mapped perturbed genes highlighted important hubs in the major subnetwork showing that EMT-Calcium processes might be "interregulated" with the stemness behaviors. First, a significant overlap among the EMT-Calcium and ESC gene sets was noticed (Fig. 6A and Supplementary Fig. S6A and B). Second, some of the perturbed genes such as *CD47*, *Notch2*, *TPM3*, and *NFYB* resided as significant hubs linking the EMT-Calcium and ESC interactions. However, despite the genes such as *ACTA1*, *CAV*, *CASP3*, *ESR1*, *EGFR*, *SP1*, and *TP53* were likewise connecting other intermodular hubs, we did not find significant changes of gene activity. To further study the possible mechanisms involved in S100A4-mediated stemness and tumorigenic properties, we showed that knockdown of S100A4 decreased *Notch2* and *PI3K/pAkt* expression and increased *PTEN* expression in HNSCCs (Fig. 6B and Supplementary Fig. S6A and B). These results suggested that *Notch* and *PTEN/PI3K/Akt* signaling played a significant role in mediating CIC characteristics; moreover, S100A4 might interregulate to modulate such HN-CIC behaviors.

Table 4. Coexpression profiles between S100A4 and Nanog, Oct-4, or CD133 of 34 HNSCC patients was examined immunohistochemically

		S100A4	
		Negative	Positive
Nanog[a]	Negative	23% (8/34)	9% (3/34)
	Positive	9% (3/34)	59% (20/34)
Oct-4[b]	Negative	23% (8/34)	9% (3/34)
	Positive	12% (4/34)	56% (19/34)
CD133[c]	Negative	21% (7/34)	15% (5/34)
	Positive	18% (6/34)	46% (16/34)

[a] $P < 0.001$ Fisher extract test.
[b] $P < 0.005$ Fisher extract test.
[c] $P = 0.138$ Fisher extract test.

Discussion

In the present study, we directly evaluated the role of S100A4 in the maintenance of stemness characteristics and tumorigenic potential of HNSCCs by lentiviral shRNAi-mediated knockdown and lentiviral-mediated overexpression of S100A4 (Figs. 2–4). Depletion of S100A4 decreased the stemness properties of HNSCCs and HN-CICs, both *in vitro*

Downloaded from cancerres.aacrjournals.org on March 23, 2011
Copyright © 2011 American Association for Cancer Research

Published OnlineFirst December 17, 2010; DOI:10.1158/0008-5472.CAN-10-2350

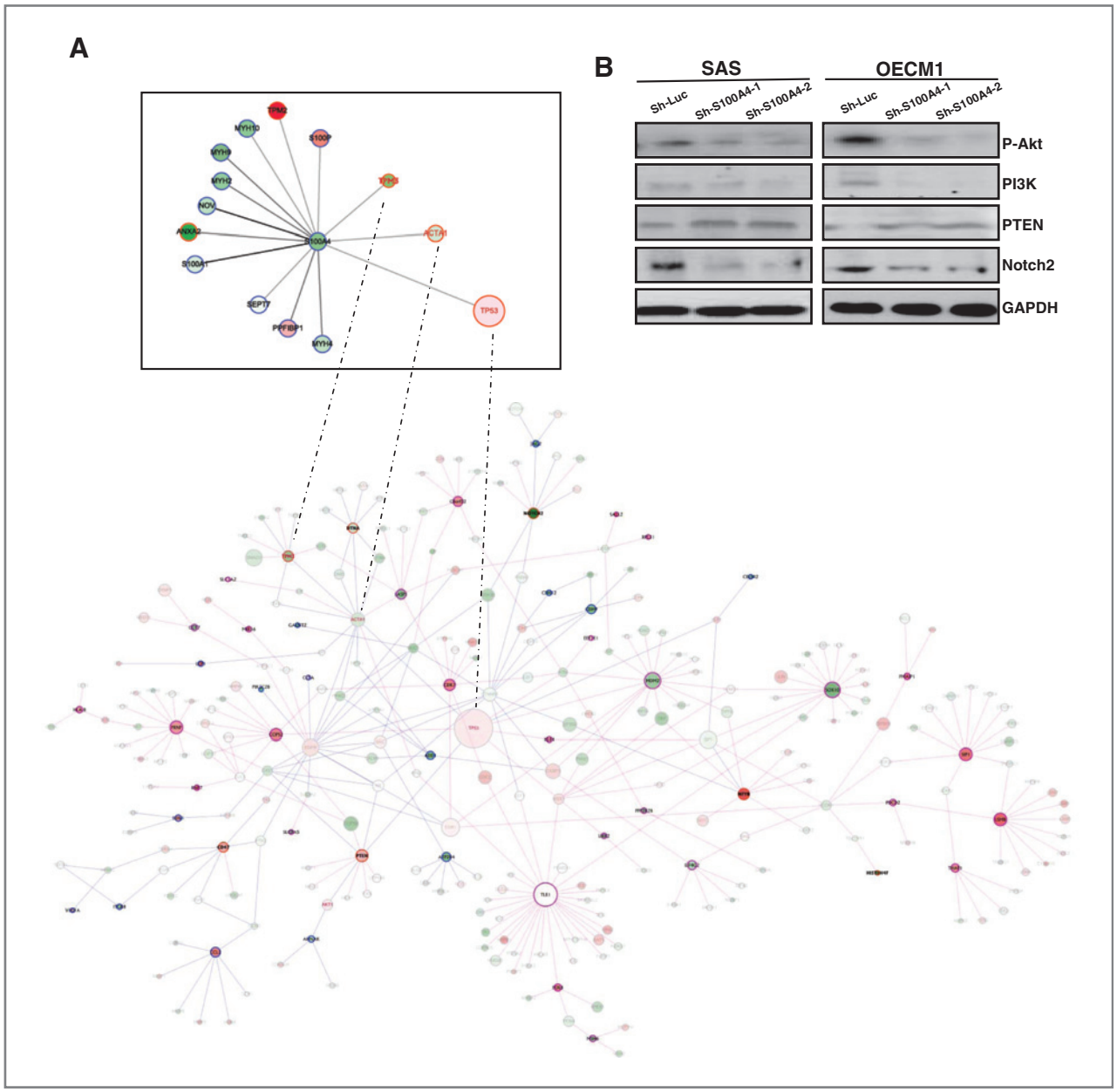

Figure 6. S100A4 knockdown affects molecular mechanisms involved in developmental (*Notch2*) and cell survival (*PTEN*/*PI3K*/*Akt*) signaling pathways. A, major subnetwork of first- and second-order neighbors of significantly perturbed genes after shRNAi-mediated knockdown of S100A4. Node coloring indicates gene activities. Red, induced; green, suppressed; node size, number of neighbor genes; node border and edge coloring, gene sets—pink, ESC; blue, EMT-Calcium; and orange, both. Neighbor genes of S100A4 are illustrated in the inset. B, total proteins from Sh-Luc- and Sh-S100A4–expressing HNSCCs were prepared and analyzed by immunoblotted with anti-Notch2, anti-PTEN, anti-pAKT, anti-PI3K, or anti-GAPDH antibodies as indicated.

and *in vivo* (Figs. 2 and 3). In contrast to S100A4-knockdown experiments, overexpression of S100A4 enhances tumor sphere-forming capability, increases the number of SP cells, and promotes migration/invasion ability of HNSCCs (Fig. 4). Furthermore, analysis of the cell survival and differentiation ability of isolated HN-CICs revealed that loss of S100A4 caused a reduction in the CIC subpopulation and an increase in the apoptotic and differentiated cells in HN-CICs (Fig. 2). Knockdown of S100A4 also lessened tumor-initiating activity (Fig. 3). These results indicate that S100A4 directly contributes to the self-renewal and survival of HN-CICs. In addition, our clinical data indicate that higher S100A4 expression correlates with HNSCC tumor progression and lymph node metastasis and contributes to patient mortality and relapse (Fig. 6). Of note, the expression profile of S100A4 is significantly correlated with stemness marker such as Nanog and Oct-4 but not CD133 (Table 4) in HNSCC. All of these suggest that stemness properties mediated by S100A4 indeed play instrumental roles

Downloaded from cancerres.aacrjournals.org on March 23, 2011
Copyright © 2011 American Association for Cancer Research

Published OnlineFirst December 17, 2010; DOI:10.1158/0008-5472.CAN-10-2350

in the tumorigenicity of HNSCC. Finally, through transcriptome-profiling analysis again, we discovered that knockdown of S100A4 affected EMT-Calcium-ESC related genes such as TP53, *Notch2*, *PTEN*, and *PI3K* (Fig. 6). The *Notch* and *PTEN/PI3K/Akt* signaling pathways have been shown for regulating self-renewal and tumorigenicity of SCs/CSCs. Although the precise role of S100A4 in *Notch2*, and *PTEN/PI3K/Akt* signaling within cancer cells, remains to be elucidated, we are the first group to show that S100A4 regulates *Notch2* and *PTEN/PI3K/Akt* expression. We further extended findings by Harris and colleagues that S100A4 is significantly upregulated not only in glioma CSCs cells (20) but also in HN-CICs. Together, all these findings highlight the importance of aberrant expression of S100A4 in neoplastic process and upregulation of S100A4 plays an important role in CSC theory.

We found more nuclear and cytoplasmic staining of *S100A4* in the moderately to poorly differentiated HNSCC tissues (Fig. 5A). Grigorian and colleagues and Fernandez-Fernandez and colleagues have shown that S100A4 directly interacts with P53 after Ca^{2+} binding (44, 45). Lin and colleagues report that *P53* negatively regulates the transcriptional activity of stem cell marker, Nanog (46). We also found that the S100A4 promoter was most hypermethylated in HNSCCs but hypomethylated in our enriched HN-CICs (data not shown). Therefore, our current hypothesis is that epigenetic modifications of the promoter region of *S100A4* gene regulates S100A4 expression; consequently, S100A4 plus Ca^{2+} abrogates the negative regulation of P53 on Nanog to enhance the expression of Nanog. Overall, future research delineates the details of how S100A4 regulates its downstream targets, and how these interactions influence the stemness properties of CSC remains to be determined.

As being a known CIC markers of HNSCC (47), it was also important to acknowledge the relative position of *CD44* in the EMT-Calcium-ESC networks. *CD44*, ranked as the 104th cut-node (out of 208) in the Ca^{2+}-EMT networks, was connected with the *EGFR*, *MMP1*, and *VCAN* in the first- and second-order connecting subnetworks. However, we did not find significant changes of *CD44* after S100A4 knockdown. We speculated that inconsistent trends between different splice variants of *CD44* (48) or alternative routing in calcium signaling pathways, different from S100A4, might be possible explanations (49). Further research effort is needed in this area.

Together, our present research showed that the S100A4 signaling pathways play a major role in the maintenance of HN-CICs population and targeting S100A4 signaling might be a potential therapeutic target for HNSCC by eliminating CICs. In addition, expression of S100A4 should be a useful prognostic factor for HNSCC patients.

Disclosure of Potential Conflicts of Interest

No potential conflicts of interest were disclosed.

Acknowledgment

The authors thank Dr. K.W. Chang (Institute of Oral Biology, National Yang-Ming University) for providing critical comment.

Grant Support

This study was supported by research grants from National Science Council (NSC95N444 and NSC97N456), Taipei VGH (V95E2007, V95B2013, V96ER2016, V97ER2018, V98ER2018, and VGHUST99-P6-39), and National Yang-Ming University (Ministry of Education, Aim for the Top University Plan: 96ADD122, 96ADD125, 96ADT191, 97ACD113, 97ACT302, and 98ACT302) in Taiwan, ROC.

The costs of publication of this article were defrayed in part by the payment of page charges. This article must therefore be hereby marked *advertisement* in accordance with 18 U.S.C. Section 1734 solely to indicate this fact.

Received June 28, 2010; revised November 3, 2010; accepted November 30, 2010; published OnlineFirst December 17, 2010.

References

1. Rosen JM, Jordan CT. The increasing complexity of the cancer stem cell paradigm. Science 2009;324:1670–3.
2. Polyak K, Weinberg RA. Transitions between epithelial and mesenchymal states: acquisition of malignant and stem cell traits. Nat Rev Cancer 2009;9:265–73.
3. Rich JN. Cancer stem cells in radiation resistance. Cancer Res 2007;67:8980–4.
4. Li X, Lewis MT, Huang J, Gutierrez C, Osborne CK, Wu MF, et al. Intrinsic resistance of tumorigenic breast cancer cells to chemotherapy. J Natl Cancer Inst 2008;100:672–9.
5. Chiou SH, Yu CC, Huang CY, Lin SC, Liu CJ, Tsai TH, et al. Positive correlations of Oct-4 and Nanog in oral cancer stem-like cells and high-grade oral squamous cell carcinoma. Clin Cancer Res 2008;14:4085–95.
6. Gupta GP, Massague J. Cancer metastasis:building a framework. Cell 2006;127:679–95.
7. DiMeo TA, Anderson K, Phadke P, Fan C, Perou CM, Naber S, et al. A novel lung metastasis signature links Wnt signaling with cancer cell self-renewal and epithelial-mesenchymal transition in basal-like breast cancer. Cancer Res 2009;69:5364–73.
8. Mani SA, Guo W, Liao MJ, Eaton EN, Ayyanan A, Zhou AY, et al. The epithelial-mesenchymal transition generates cells with properties of stem cells. Cell 2008;133:704–15.
9. Morel AP, Lievre M, Thomas C, Hinkal G, Ansieau S, Puisieux A. Generation of breast cancer stem cells through epithelial-mesenchymal transition. PLoS One 2008;3:e2888.
10. Stein U, Arlt F, Walther W, Smith J, Waldman T, Harris ED, et al. The metastasis-associated gene S100A4 is a novel target of beta-catenin/T-cell factor signaling in colon cancer. Gastroenterology 2006;131:1486–500.
11. Ito M, Kizawa K. Expression of calcium-binding S100 proteins A4 and A6 in regions of the epithelial sac associated with the onset of hair follicle regeneration. J Invest Dermatol 2001;116:956–63.
12. Mazzucchelli L. Protein S100A4: too long overlooked by pathologists? Am J Pathol 2002;160:7–13.
13. Morris RJ, Liu Y, Marles L, Yang Z, Trempus C, Li S, et al. Capturing and profiling adult hair follicle stem cells. Nat Biotechnol 2004;22:411–7.
14. Tumbar T, Guasch G, Greco V, Blanpain C, Lowry WE, Rendl M, et al. Defining the epithelial stem cell niche in skin. Science 2004;303:359–63.
15. Grum-Schwensen B, Klingelhofer J, Berg CH, El-Naaman C, Grigorian M, Lukanidin E, et al. Suppression of tumor development and metastasis formation in mice lacking the S100A4(mts1) gene. Cancer Res 2005;65:3772–80.
16. Grigorian M, Ambartsumian N, Lykkesfeldt AE, Bastholm L, Elling F, Georgiev G, et al. Effect of mts1 (S100A4) expression on the

Downloaded from cancerres.aacrjournals.org on March 23, 2011
Copyright © 2011 American Association for Cancer Research

Published OnlineFirst December 17, 2010; DOI:10.1158/0008-5472.CAN-10-2350

progression of human breast cancer cells. Int J Cancer 1996;67:831–41.
17. Saleem M, Kweon MH, Johnson JJ, Adhami VM, Elcheva I, Khan N, et al. S100A4 accelerates tumorigenesis and invasion of human prostate cancer through the transcriptional regulation of matrix metalloproteinase 9. Proc Natl Acad Sci U S A 2006;103:14825–30.
18. Mahon PC, Baril P, Bhakta V, Chelala C, Caulee K, Harada T, et al. S100A4 contributes to the suppression of BNIP3 expression, chemoresistance, and inhibition of apoptosis in pancreatic cancer. Cancer Res 2007;67:6786–95.
19. Chaerkady R, Kerr CL, Kandasamy K, Marimuthu A, Gearhart JD, Pandey A. Comparative proteomics of human embryonic stem cells and embryonal carcinoma cells. Proteomics 2010;10:1359–73.
20. Harris MA, Yang H, Low BE, Mukherjee J, Guha A, Bronson RT, et al. Cancer stem cells are enriched in the side population cells in a mouse model of glioma. Cancer Res 2008;68:10051–9.
21. Davies BR, O'Donnell M, Durkan GC, Rudland PS, Barraclough R, Neal DE, et al. Expression of S100A4 protein is associated with metastasis and reduced survival in human bladder cancer. J Pathol 2002;196:292–9.
22. Gongoll S, Peters G, Mengel M, Piso P, Klempnauer J, Kreipe H, et al. Prognostic significance of calcium-binding protein S100A4 in colorectal cancer. Gastroenterology 2002;123:1478–84.
23. Rudland PS, Platt-Higgins A, Renshaw C, West CR, Winstanley JH, Robertson L, et al. Prognostic significance of the metastasis-inducing protein S100A4 (p9Ka) in human breast cancer. Cancer Res 2000;60:1595–603.
24. Lee J, Kotliarova S, Kotliarov Y, Li A, Su Q, Donin NM, et al. Tumor stem cells derived from glioblastomas cultured in bFGF and EGF more closely mirror the phenotype and genotype of primary tumors than do serum-cultured cell lines. Cancer Cell 2006;9:391–403.
25. Futschik ME, Carlisle B. Noise-robust soft clustering of gene expression time-course data. J Bioinf Comput Biol 2005;3:965–88.
26. Dennis G Jr, Sherman BT, Hosack DA, Yang J, Gao W, Lane HC, et al. DAVID: Database for Annotation, Visualization, and Integrated Discovery. Genome Biol 2003;4:P3.
27. Smyth GK. Linear models and empirical Bayes methods for assessing differential expression in microarray experiments. Stat Appl Genet Mol Biol 2004;3:article 3.
28. Strimmer K. A unified approach to false discovery rate estimation. BMC Bioinf 2008;9:303.
29. Yu YH, Kuo HK, Chang KW. The evolving transcriptome of head and neck squamous cell carcinoma: a systematic review. PLoS One 2008;3:e3215.
30. Ben-Porath I, Thomson MW, Carey VJ, Ge R, Bell GW, Regev A, et al. An embryonic stem cell-like gene expression signature in poorly differentiated aggressive human tumors. Nat Genet 2008;40:499–507.
31. Muller FJ, Laurent LC, Kostka D, Ulitsky I, Williams R, Lu C, et al. Regulatory networks define phenotypic classes of human stem cell lines. Nature 2008;455:401–5.
32. Peri S, Navarro JD, Amanchy R, Kristiansen TZ, Jonnalagadda CK, Surendranath V, et al. Development of human protein reference database as an initial platform for approaching systems biology in humans. Genome Res 2003;13:2363–71.
33. Gentleman RC, Carey VJ, Bates DM, Bolstad B, Dettling M, Dudoit S, et al. Bioconductor: open software development for computational biology and bioinformatics. Genome Biol 2004;5:R80.
34. Shannon P, Markiel A, Ozier O, Baliga NS, Wang JT, Ramage D, et al. Cytoscape: a software environment for integrated models of biomolecular interaction networks. Genome Res 2003;13:2498–504.
35. Ginestier C, Hur MH, Charafe-Jauffret E, Monville F, Dutcher J, Brown M, et al. ALDH1 is a marker of normal and malignant human mammary stem cells and a predictor of poor clinical outcome. Cell Stem Cell 2007;1:555–67.
36. Schafer BW, Heizmann CW. The S100 family of EF-hand calcium-binding proteins: functions and pathology. Trends Biochem Sci 1996;21:134–40.
37. Schafer BW, Wicki R, Engelkamp D, Mattei MG, Heizmann CW. Isolation of a YAC clone covering a cluster of nine S100 genes on human chromosome 1q21: rationale for a new nomenclature of the S100 calcium-binding protein family. Genomics 1995;25:638–43.
38. Engelkamp D, Schafer BW, Mattei MG, Erne P, Heizmann CW. Six S100 genes are clustered on human chromosome 1q21: identification of two genes coding for the two previously unreported calcium-binding proteins S100D and S100E. Proc Natl Acad Sci U S A 1993;90:6547–51.
39. Visvader JE, Lindeman GJ. Cancer stem cells in solid tumours: accumulating evidence and unresolved questions. Nat Rev Cancer 2008;8:755–68.
40. Dean M, Fojo T, Bates S. Tumour stem cells and drug resistance. Nat Rev Cancer 2005;5:275–84.
41. Bleau AM, Hambardzumyan D, Ozawa T, Fomchenko EI, Huse JT, Brennan CW, et al. PTEN/PI3K/Akt pathway regulates the side population phenotype and ABCG2 activity in glioma tumor stem-like cells. Cell Stem Cell 2009;4:226–35.
42. Moriyama-Kita M, Endo Y, Yonemura Y, Heizmann CW, Schäfer BW, Sasaki T, et al. Correlation of S100A4 expression with invasion and metastasis in oral squamous cell carcinoma. Oral Oncol 2004;40:496–500.
43. Sapkota D, Bruland O, Boe OE, Bakeer H, Elgindi OA, Vasstrand EN, et al. Expression profile of the S100 gene family members in oral squamous cell carcinomas. J Oral Pathol Med 2008;37:607–15.
44. Fernandez-Fernandez MR, Veprintsev DB, Fersht AR. Proteins of the S100 family regulate the oligomerization of p53 tumor suppressor. Proc Natl Acad Sci U S A 2005;102:4735–40.
45. Grigorian M, Andresen S, Tulchinsky E, Kriajevska M, Carlberg C, Kruse C, et al. Tumor suppressor p53 protein is a new target for the metastasis-associated Mts1/S100A4 protein: functional consequences of their interaction. J Biol Chem 2001;276:22699–708.
46. Lin T, Chao C, Saito S, Mazur SJ, Murphy ME, Appella E, et al. p53 induces differentiation of mouse embryonic stem cells by suppressing Nanog expression. Nat Cell Biol 2005;7:165–71.
47. Prince ME, Sivanandan R, Kaczorowski A, Wolf GT, Kaplan MJ, Dalerba P, et al. Identification of a subpopulation of cells with cancer stem cell properties in head and neck squamous cell carcinoma. Proc Natl Acad Sci U S A 2007;104:973–8.
48. Mack B, Gires O. CD44s and CD44v6 expression in head and neck epithelia. PLoS One 2008;3:e3360.
49. Wang SJ, Bourguignon LY. Hyaluronan and the interaction between CD44 and epidermal growth factor receptor in oncogenic signaling and chemotherapy resistance in head and neck cancer. Arch Otolaryngol Head Neck Surg 2006;132:771–8.

Downloaded from cancerres.aacrjournals.org on March 23, 2011
Copyright © 2011 American Association for Cancer Research